

Huedayi Korkusuz  
Philip Esters  
Nagy Naguib  
N.-E. Nour Eldin  
Sebastian Lindemayr  
Frank Huebner  
Ahmed Koujan  
Reinhold Bug  
Hanns Ackermann  
Thomas J. Vogl

## Acute myocarditis in a rat model: late gadolinium enhancement with histopathological correlation

Received: 14 October 2008  
Revised: 17 March 2009  
Accepted: 26 March 2009  
Published online: 21 May 2009  
© European Society of Radiology 2009

H. Ackermann  
Department of Biomathematics,  
Johann Wolfgang Goethe-University  
Hospital Frankfurt,  
Theodor-Stern-Kai 7,  
60590 Frankfurt, Germany

H. Korkusuz (✉) · P. Esters ·  
N. Naguib · N.-E. Nour Eldin ·  
S. Lindemayr · F. Huebner · A. Koujan ·  
T. J. Vogl  
Department of Diagnostic  
and Interventional Radiology,  
Johann Wolfgang Goethe University  
Frankfurt,  
Theodor-Stern-Kai 7,  
60590 Frankfurt, Germany  
e-mail: huedayi.korkusuz@kgu.de  
Tel.: +49-069-630187280  
Fax: +49-069-630183594

R. Bug  
Senckenberg Institute of Pathology,  
Johann Wolfgang Goethe University  
Hospital Frankfurt,  
Theodor-Stern-Kai 7,  
60590 Frankfurt, Germany

**Abstract** The aim of the current study was to use an established animal model of autoimmune myocarditis and to judge the ability of cardiovascular MRI (CMR) in quantitatively measuring the extent of myocardial involvement compared with histopathological measurement of severity and extent. Experimental autoimmune myocarditis (EAM) was induced in 10 male Lewis rats. On day 21, all animals were investigated by CMR to measure the extent of late gadolinium enhancement (LGE). Subsequently, histopathological evaluation of the entire heart was performed. All animals of the experimental group fulfilled histopathological

criteria of myocarditis, revealing necrosis in seven of eight cases. At reduced heart rate, area of LGE correlated highly with histologically proven area of myocarditis ( $r=0.80-0.87$ ,  $p<0.05$ ). LGE was mainly located in the anterior (range 50–62.5%) and lateral (range 62.5–75%) left ventricular wall and septum (range 25–50%) with a midwall to subepicardial accentuation. The LGE pattern found by CMR can be regarded as suggestive of EAM. With cellular necrosis being the main mechanism for LGE we were able to show high correlations between CMR examination results and histopathologically proven areas of myocarditis. Thus we think the current animal model can provide the opportunity for further fundamental research into myocarditis.

**Keywords** Myocarditis · Animal · MRI

### Introduction

Myocarditis is defined as myocardial inflammation associated with edema, cellular infiltration, apoptosis and necrosis of cardiomyocytes [1]. Myocarditis was found in the autopsy of 16–21% of children with sudden cardiac death [2]. The clinical presentation of myocarditis varies from asymptomatic to nonspecific symptoms (arrhythmia, angina pectoris, sudden cardiac death) making its diagnosis difficult.

Despite innovations in diagnostics, a definitive diagnosis of myocarditis still requires an invasive image-guided endomyocardial biopsy (EMB). As the myocardial inflam-

mation pattern of myocarditis may be diffuse or focal, the so-called sampling error leads to very low sensitivity of EMB of about 20% [3]. As alternatives to EMB, noninvasive methods such as cardiovascular magnetic resonance imaging (CMR) have gained increasing interest [4–7]. Late gadolinium enhancement (LGE) with an intramyocardial to subepicardial accentuated pattern is considered to be highly suggestive of myocardial inflammation [4, 7, 8]. Compared with EMB, sensitivity and specificity of CMR lie between 90 and 100% [4]. Nevertheless these figures result from clinical studies verifying myocarditis by EMB. Fundamental research using an animal model with the

possibility of histopathological examination of the whole myocardium has not been published to date. Furthermore, the important issue of correlating the enhancement with the histologically proven extent of myocarditis has not yet been investigated.

Experimental autoimmune myocarditis (EAM) is an established animal model to display myocarditis [9–11] as its histomorphology is similar to human myocarditis [12–14]. The aim of the current study was to establish an animal model for CMR imaging research and to judge the ability of CMR in quantitatively measuring the extent of myocardial involvement compared with histopathological measurement of severity and extent.

## Methods

### Immunization of animals

Twenty male Lewis rats, aged 6–8 weeks, weighing 250–300 g were used in this study. All experiments were approved by the governmental committee and our institutional animal research review board.

According to the established EAM model [12] 10 animals served as the experimental group and were immunised with porcine cardiac myosine (PCM; Sigma Aldrich, M0531); the remaining 10 animals served as control. The allocation to the control or experimental group was done by random selection.

PCM was diluted with phosphate-buffered saline (PBS, BD Heidelberg, Germany) and finally emulsified with complete Freud's adjuvant (CFA; BD Heidelberg, Germany) 1:1. On days 1 and 7 experimental group rats were subcutaneously injected in the footpad with 0.5 ml PCM-CFA emulsion, containing 1 mg PCM. Control group animals were subcutaneously injected with 0.25 ml CFA only, i.e. without PCM.

### CMR sequences and procedure

On day 21, animals were examined by ECG-triggered CMR (1.5 T, Magnetom Sonata Siemens, Erlangen, Germany) under isoflurane anaesthesia (2.2% isoflurane in air). Isoflurane anaesthesia was used due to its negative inotropic effect [15].

Animals were positioned headfirst, supine. ECG electrodes were placed on the animal's pads and a finger surface radiofrequency coil, serving as receiver, was fixed on the animal's chest.

Slice levels were adjusted to the individual heart axis and images of the horizontal long axis (4-chamber-view) and short axis were performed by a turboFLASH imaging sequence (turbo fast low angle shot, TFL). These fast gradient echo (GRE) sequences deliver T1-weighted images using the inversion recovery technique with low

angle shots. Determination of inversion time in short-axis sequences was performed by a scout (inversion time scout) 10 min after intravenous injection of gadolinium-DTPA (Magnevist®; 0.1 mmol/kg), as recommended in the literature [16]. At ideal inversion time, MR scout images show dark, healthy myocardium in contrast to a bright blood pool.

Using the previously determined TI, animals were examined by using GRE sequences in a high resolution 2D fashion without and with fat suppression. GRE imaging was performed with and without fat suppression to improve the topographic mapping of myocarditis by eliminating the high fat signal ratio by increasing the contrast for visualizing the area of myocarditis. CMR examination was performed as follows: 15 min after Gd-DTPA injection CMR imaging started with GRE sequences without fat suppression (FoV read 120 mm, FoV phase 46.0%, slice thickness 3 mm, TR 750 ms, TE 4.38 ms, averages 2, flip angle 25°, base resolution 256, phase resolution 100%) and directly afterwards with fat suppression.

To assess a possible influence of heart rate on CMR imaging quality, 25 min after Gd-DTPA injection heart rate was reduced to 90–120 bpm by injection of propofol and metoprolol, and GRE sequences first without (Fig. 1a) and then with fat suppression were repeated.

Subsequently, animals were sacrificed by propofol overdose and turbo spin echo (TSE) sequences (FoV read 100 mm, FoV phase 57.8%, slice thickness 2 mm, TR 742 ms, TE 17 ms, averages 3, flip angle 180°, fat saturated, base resolution 448, phase resolution 100%) of the arrested heart were performed, 30 min after Gd-DTPA injection (Fig. 1b) to achieve a higher signal-to-noise ratio.

CMR images were analysed using a commercially available PACS system (Centricity, GE Healthcare, Chicago, USA) by two radiologists with 5 and 8 years experience in the field of cardiac MRI in consensus. LGE was traced by manual drawing of regions of interest (ROIs) around the enhanced areas. The size of LGE was expressed as a percentage of the total segment for each slice. As we could not be sure to perform the CMR examination in the same phase of the cardiac cycle for each animal and additionally due to variation of animals regarding heart size and weight, the expression of LGE as a percentage of the total segment seems to be the optimal method for evaluation rather than absolute figures of LGE. Percentages of LGE were measured in three representative slices from base to apex and summed for each animal.

In order to investigate the LGE distribution, the right and left ventricle were divided into six segments in order to specify LGE location.

### Histopathological preparations and analysis

After CMR the heart was explanted by thoracotomy, then fixed in formalin (4%) for 6 h and finally dehydrated.

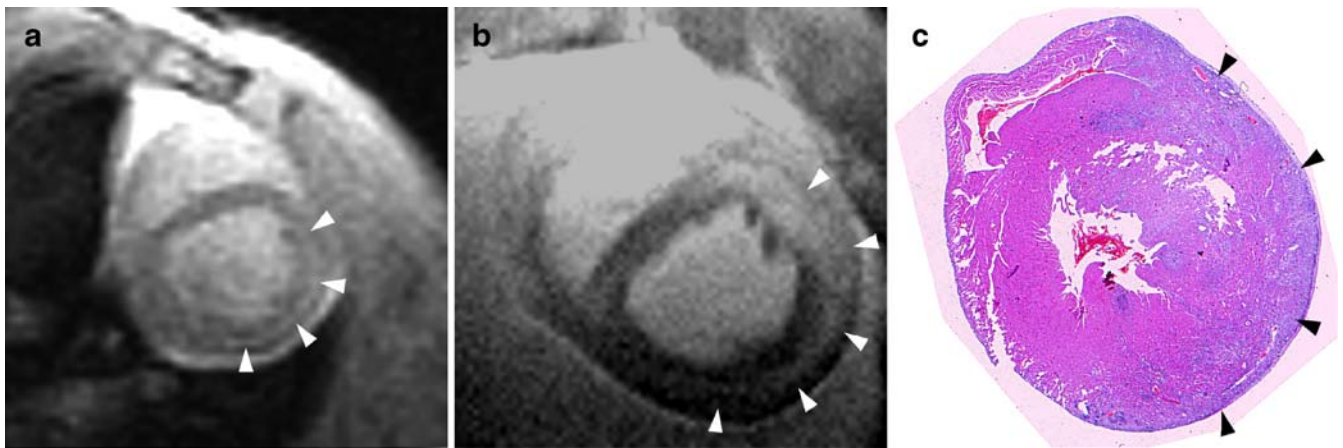


**Fig. 1** CMR images (a, b) in one animal of the experimental group and histological findings for the same animal (c). **a** GRE sequence without fat saturation at reduced heart rate, 25 min after gadolinium injection. Arrows indicate area of late gadolinium enhancement in the anterior and lateral left ventricular wall. **b** TSE sequence shows

late enhancement (arrows) in the anterior and lateral wall of left ventricle, 30 min after gadolinium injection. **c** Histological findings demonstrate subepicardial to midwall cellular infiltration by leucocytes in the anterior and lateral left ventricular wall (black arrows)

For paraffin embedding and sections, 2-mm-thick slices were prepared from the formalin-fixed myocardium. On the following day tissue was effused in paraffin and stored at 21°C. A microtome was then used to afford 5- $\mu$ m-thick slices, which were transferred into warm water and placed on a slide. Hematoxylin–eosin (HE) staining was used.

Macroscopy of rat hearts was evaluated by assigning a macroscopic score according to Yuan et al. [17], regarding macroscopic morphology and pericardial effusion (*macroscopic morphology*, 0=no inflammatory alteration; 1=focal inflammatory signs; 2=multiple/diffuse inflammatory signs less than or equal to one third of heart size; 3=diffuse inflammatory signs greater than one third of heart size; *pericardial effusion*, 0=no effusion; 1=mild effusion; 2=massive effusion).

The severity of myocarditis was histologically analysed and the results were based on a microscopic score system according to the following histological criteria: density of inflammatory infiltration (graded 0–3) defined by presence of leucocytes, strength of inflammatory destruction with rarefaction and pushing apart of heart muscle fibres (graded 0–3), occurrence of pericarditis (graded 0–2), occurrence of necrosis (graded 0–3). Degree of necrosis was defined according to Kanda et al. [18] as: grade 0, no necrosis; grade 1, necrosis involving less than 25% of the ventricular myocardium; grade 2, necrosis involving 25–50% of the myocardium; grade 3, necrosis involving more than 50% of the myocardium. Results were pooled into a microscopic score system, with a maximum score of 11 points, to express severity of myocarditis.

Areas of infiltration were measured in slices from the base to apex of the heart by using dedicated software (analySIS® 5.0, Soft Imaging System, Münster, Germany). Infiltrated areas were bordered manually, each in a representative slice of apex, mid and base of the heart in a way similar to ROI drawing in CMR.

To analyse the location of histological infiltration we used the identical ventricular segment model employed for encoding of LGE location.

#### Statistical analysis

All statistical analyses were calculated with biostatistical software (SPSS® 12.0 for Windows, SPSS Inc., Chicago, Illinois, USA and BiAS for Windows 8.6) Percentages of LGE areas and histologic inflammation areas are expressed as means  $\pm$  standard deviation (SD). Correlations between LGE area size in images and histological inflammatory area were calculated by using the Bland–Altman correlation test. Median scores for histopathology and CME were calculated, because the scores have ordinal scales. The Mann–Whitney *U* test was used to detect significant differences in evaluating the extent of late gadolinium enhancement at physiological and reduced heart rate. Results were considered to be significant at  $p < 0.05$ .

## Results

On day 21, we examined animals by CMR. Two animals of the experimental group died on days 15 and 17 and consequently could not be examined on day 21 by CMR; those animals were assigned a macroscopic score of 5 and a microscopic score of 11.

#### CMR examinations

As mentioned before, only eight experimental and all control group animals ( $n=10$ ) were examined by CMR, using GRE and TSE sequences, on day 21. In general, LGE

was detectable in CMR images of experimental animals, but in none of the control group animals.

#### Analysis of GRE examination

Beginning with GRE sequences without fat suppression, LGE was detectable in six of eight animals (75%); the mean percentage of LGE areas was 5.67% (SD±4.37) at physiological heart rate (280–400 bpm). At reduced heart rate (90–120 bpm) LGE was detectable in all examined experimental animals (100%); mean percentage of LGE areas was 25.93% (SD±23.6).

GRE examination with fat suppression displayed LGE in five of eight animals (62.5%) at physiological heart rate; mean percentage of LGE areas was 6.74% (SD±5.19). At reduced heart rate, LGE was detectable in all examined experimental animals (100%); mean percentage of LGE areas was 22.20% (SD±17.22).

Statistically significant difference was detected on evaluating the extent of LGE at physiological and reduced heart rate by using the Mann–Whitney *U* test, indicating extent of LGE to be higher at reduced heart rate than physiological heart rate ( $p=0.037$ ).

#### Analysis of TSE examination

TSE sequences without fat suppression detected LGE in seven of eight animals (87.5%); mean percentage of LGE areas was 5.43% (SD±6.42). In TSE sequences with fat suppression LGE was found in six of eight animals (75%); mean percentage of LGE areas was 5.74% (SD±7.0).

#### Distribution of LGE

Independent of the examined CMR sequence (GRE vs. TSE) LGE was mostly localized in the myocardium of the left ventricle, anterior (range 50–62.5%) and lateral (range 62.5–75%), and in the septum (range 25–50%), according to the ventricular segmental model; inside the myocardium, LGE was predominantly found midwall and subepicardial, and in no case subendocardial or transmural (Fig. 2).

#### Histopathological analysis

All remaining animals of the experimental group ( $n=8$ ) developed myocarditis according to the described microscopic score system, whereas control group animals ( $n=10$ ) were histopathologically healthy.

In seven of eight animals of the experimental group we found pericardial effusion and visible signs of inflammation. Median macroscopic score was 4.5 (range 0–5) in the experimental group and 0 (range 0–1) in the control group.

Experimental group animals had a mainly high density of inflammatory infiltration with a subepicardial accentuation. Heart muscle fibres were destroyed and pushed apart as a result of inflammation. Necrosis was observed in seven of eight animals of the experimental group. The degree of necrosis detected in the experimental group by histopathological examination was graded from 0 to 3 (Table 1).

Control group animals showed histologically unchanged, healthy myocardium. Median microscopic score was 9 (range 1–11) in the experimental group and 0 (range 0) in the control group.

#### Correlation of CMR examination and histology

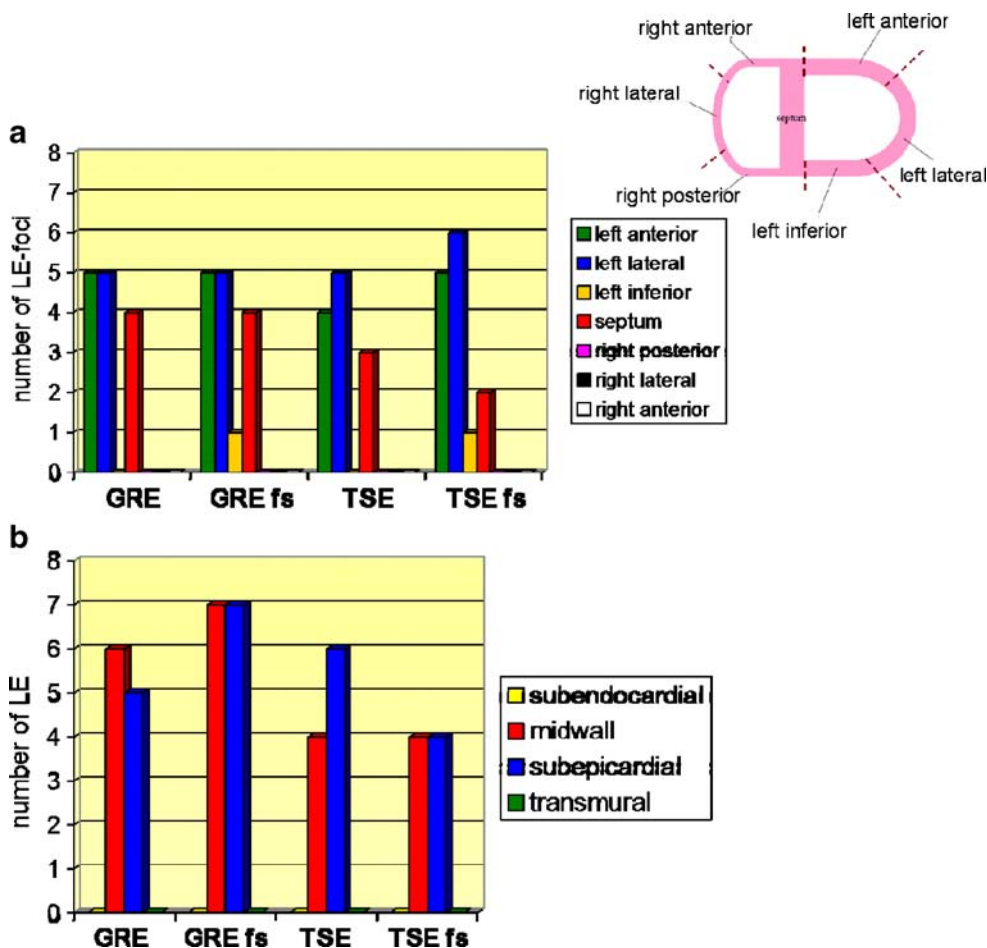
Comparing mean percentages of LGE areas in CMR images and percentage of histological areas of inflammation, we found high correlations (Bland–Altman correlation test) for GRE examination at reduced heart rate (correlation coefficient=0.80,  $p=0.02$ ), for GRE examination with fat saturation at reduced heart rate (correlation coefficient=0.87,  $p=0.005$ ), for TSE examination (correlation coefficient=0.81,  $p=0.01$ ) and for TSE examination with fat saturation (correlation coefficient=0.73,  $p=0.04$ ) (Table 2). There was no significant correlation for GRE examination at physiological heart rate (Table 2).

## Discussion

CMR has been established for a long time, especially in evaluating myocardial infarction and differentiating viable and nonviable myocardium [19]. In diagnosing myocardial inflammation, CMR has gained interest due to the disadvantages of EMB [4, 5, 7]. Hypotheses concerning the molecular pathophysiology of late gadolinium enhancement have been provided based on necrotic cardiomyocytes. As found in experimental animals, the necrotic cardiomyocytes with ruptured membranes are able to take up contrast media such as gadolinium-DTPA, whereas gadolinium as an extracellular molecule cannot penetrate into healthy cardiomyocytes, resulting in contrast media enhancement of necrotic foci. This conclusion is also agreed by Friedrich et al. [20].

LGE patterns have been described for myocardial infarction and for myocardial inflammation [4, 7, 8]. Several studies verified a subendocardial accentuated LGE pattern as typical for myocardial infarction by comparing CMR examination with histological findings in experimental animal models of myocardial infarction [21]. To our knowledge no study comparing CMR findings with histological findings in experimental animal models of myocardial inflammation has been published. Consequently, described LGE patterns probably indicating myocardial inflammation, as well as data for sensitivity and

**Fig. 2** LGE distribution in the left and right ventricle at reduced heart rate (a) and inside the myocardial wall (b). Frequencies of LGE foci are indicated as “number of LGE” on the y-axis. GRE sequence without fat suppression (GRE), GRE sequence with fat suppression (GRE fs), TSE sequence without fat suppression (TSE), TSE sequence with fat suppression (TSE fs)



specificity of CMR, still have to be verified by comparing CMR and histology.

As described before, LGE was only detectable in experimental group animals and the extent of LGE areas correlated highly with histological inflammation. Even the lack of a nonclinical high-field MR magnet seems to be no barrier to perform CMR imaging in small rodents, in agreement with Gilson and Kraitchman [16]. All animals of the experimental group revealed LGE in GRE sequences at reduced heart rate. Even animals with minimal histological changes (histopathological score 1 and 2) revealed LGE.

**Table 1** Degree of necrosis detected by histopathological examination in the experimental group

Degree of necrosis	Number of rats	Percentage
Grade 0	1	12.5
Grade 1	4	50
Grade 2	1	12.5
Grade 3	2	25

Grade 0, no necrosis; grade 1, necrosis involving less than 25% of the ventricular myocardium; grade 2, necrosis involving 25–50% of the myocardium; grade 3, necrosis involving more than 50% of the myocardium

The rat heart rates during CMR examination at physiological heart rate varied from 280 to 370 bpm. This heart rate diversity might be a reason why some of the experimental animals did not reveal LGE in GRE sequences at physiological heart rate, but at reduced heart rate (all animals < 120 bpm) showed LGE.

Concerning influence of heart rate on CMR image quality, examined mean percentage of LGE areas in GRE examination was higher at reduced heart rate than at physiological heart rate (Fig. 2). At physiological heart rate

**Table 2** Correlation between extent of LGE and histologically proven area of inflammation

CMR sequence	Bland–Altman correlation coefficient (pvalue)
GRE	–0.129 (0.76)
GRE, HR reduced	0.80 (0.02)
GRE with fat suppression	–0.063 (0.88)
GRE with fat suppression, HR reduced	0.87 (0.005)
TSE with fat suppression	0.728 (0.04)
TSE	0.81 (0.01)

(280–400 bpm) LGE appears to be underestimated due to more intense imaging artefacts [21]. On the other hand LGE was revealed more often at reduced heart rate than at physiological heart rate (100% vs. 62.5–75%, respectively), independent of the GRE sequences used.

We presume that smaller areas of LGE in TSE sequences compared with GRE sequences result from the long time (about 30–35 min) between injection of gadolinium and the TSE measurement. In consequence we think that more gadolinium was washed out than during the GRE measurement.

In small rodent CMR imaging a heart rate of appropriately 100 bpm should be attained to minimize imaging artefacts. To what extent a reduction of heart rate should be applied in human cardiac MRI could be evaluated by clinical studies.

Evaluating the distribution of LGE, we found a pattern in which LGE was mainly located inside the anterior and lateral left ventricular wall including septum with a midwall to subepicardial accentuation.

Comparing our results with Mahrholdt et al.'s [22], who showed that LGE patterns differ according to type of viral myocarditis (Parvovirus B19 versus human herpesvirus 6), and with Abdel-Aty et al.'s [23] we can affirm that a predominant accentuation of LGE pattern in the midwall to

subepicardial layer is highly suggestive of myocardial inflammation. Differences in LGE distribution inside myocardium can be explained by different aetiologies of myocarditis in the compared studies (viral versus autoimmune).

Compared with the LGE pattern presumed as typical for myocardial infarction with a subendocardial accentuation, the main difference seems to be the subepicardial accentuation in myocarditis.

The animal model's clinical relevance arises from its histomorphological similarity to human myocarditis [13, 14, 24].

## Conclusion

EAM in a rat model can be detected by using a clinical MR magnet. LGE located in the anterior and lateral left ventricular wall including the septum with a midwall to subepicardial accentuation seems to be a pattern suggestive of the diagnosis of myocarditis. Even though cellular necrosis is mostly accepted as the main mechanism for LGE, we were able to show high correlation between CMR examination results and histopathological findings and thus we think the current animal model can provide the opportunity for further fundamental research into myocarditis.

## References

- Skouri HN, Dec GW, Friedrich MG et al (2006) Noninvasive imaging in myocarditis. *J Am Coll Cardiol* 48:2085–2093
- Neuspiel DR, Kuller LH (1985) Sudden and unexpected natural death in childhood and adolescence. *JAMA* 254:1321–1325
- Lie JT (1988) Myocarditis and endomyocardial biopsy in unexplained heart failure: a diagnosis in search of a disease. *Ann Intern Med* 109:525–528
- Codreanu A, Djaballah W, Angioi M et al (2007) Detection of myocarditis by contrast-enhanced MRI in patients presenting with acute coronary syndrome but no coronary stenosis. *J Magn Reson Imaging* 25:957–964
- Marcu CB, Beek AM, van Rossum AC (2006) Clinical applications of cardiovascular magnetic resonance imaging. *CMAJ* 175:911–917
- Sechtem U, Mahrholdt H, Vogelsberg H (2007) Cardiac magnetic resonance in myocardial disease. *Heart (British Cardiac Society)* 93:1520–1527
- Yelgec NS, Dymarkowski S, Ganame J et al (2007) Value of MRI in patients with a clinical suspicion of acute myocarditis. *Eur Radiol* 17:2211–2217
- Stork A, Mullerleile K, Bansmann PM et al (2007) Patterns of delayed-enhancement in MRI of ischemic and non-ischemic cardiomyopathies. *Rofo* 179:21–30
- Kodama M, Tachikawa H, Kashimura T et al (2004) Effects of humoral factors on left ventricular remodeling under chronic heart failure. *Nippon yakurigaku zasshi* 123:63–70
- Veeraveedu PT, Watanabe K, Ma M et al (2008) Torasemide, a long-acting loop diuretic, reduces the progression of myocarditis to dilated cardiomyopathy. *Eur J Pharmacol* 581:121–131
- Yoshida Y, Shioi T, Izumi T (2007) Resveratrol ameliorates experimental autoimmune myocarditis. *Circ J* 71:397–404
- Kodama M, Matsumoto Y, Fujiwara M et al (1990) A novel experimental model of giant cell myocarditis induced in rats by immunization with cardiac myosin fraction. *Clin Immunol Immunopathol* 57:250–262
- Kodama M, Matsumoto Y, Fujiwara M et al (1991) Characteristics of giant cells and factors related to the formation of giant cells in myocarditis. *Circ Res* 69:1042–1050
- Kodama M, Izumi T (1991) Experimental autoimmune myocarditis. *Acta Med Biol* 39:1–10
- Davies LA, Hamilton DL, Hopkins PM et al (1999) Concentration-dependent inotropic effects of halothane, isoflurane and sevoflurane on rat ventricular myocytes. *Br J Anaesth* 82:723–730
- Gilson WD, Kraitchman DL (2007) Cardiac magnetic resonance imaging in small rodents using clinical 1.5 T and 3.0 T scanners. *Methods (San Diego, Calif)* 43:35–45
- Yuan Z, Liu Y, Liu Y et al (2004) Peroxisome proliferator-activated receptor-gamma ligands ameliorate experimental autoimmune myocarditis associated with inhibition of self-sensitive T cells. *J Cardiovasc Pharmacol* 43:868–875

- 
18. Kanda T, Takahashi T, Kudo S et al (2004) Leptin deficiency enhances myocardial necrosis and lethality in a murine model of viral myocarditis. *Life Sci* 75:1435–1447
  19. Tomlinson DR, Becher H, Selvanayagam JB (2008) Assessment of myocardial viability: comparison of echocardiography versus cardiac magnetic resonance imaging in the current era. *Heart Lung Circ* 17:173–185
  20. Friedrich MG, Abdel-Aty H, Taylor A et al (2008) The salvaged area at risk in reperfused acute myocardial infarction as visualized by cardiovascular magnetic resonance. *J Am Coll Cardiol* 51:1581–1587
  21. Saraste A, Nekolla S, Schwaiger M (2008) Contrast-enhanced magnetic resonance imaging in the assessment of myocardial infarction and viability. *J Nucl Cardiol* 15:105–117
  22. Mahrholdt H, Wagner A, Deluigi CC et al (2006) Presentation, patterns of myocardial damage, and clinical course of viral myocarditis. *Circulation* 114:1581–1590
  23. Abdel-Aty H, Boye P, Zagrosek A et al (2005) Diagnostic performance of cardiovascular magnetic resonance in patients with suspected acute myocarditis: comparison of different approaches. *J Am Coll Cardiol* 45:1815–1822
  24. Uribe S, Muthurangu V, Boubertakh R et al (2007) Whole-heart cine MRI using real-time respiratory self-gating. *Magn Reson Med* 57:606–613